STRUCTURAL ANALYSIS OF SUBASSEMBLY WRAPPER TUBES WITH THE THREE-DIMENSIONAL FINITE ELEMENT CODE KASTEN

L. H. STEINBOCK

Institut für Material- und Festkörperforschung,
Kernforschungszentrum Karlsruhe, Postfach 3640, D-7500 Karlsruhe 1, Germany

SUMMARY

1. Problem. — A mathematical model of the structural properties of a fuel element under in-pile conditions has to incorporate the wrapper tube, the fuel pins and the spacing devices between them. The finite element method is one way to build such a model because by that it is possible to connect bodies which are as different in shape as the wrapper tube, spacer grids and pins. Despite their different shapes they all may be build out of flat or curved plate elements. The first step in reaching this aim may be the code KASTEN which simulates the mechanical properties of either the wrapper tube or the fuel pin cladding.

2. Method of Solution. — The code KASTEN subdivides a tube in up to 30 axial rings of hexagonal (wrapper) or circular (clad) cross section. Each ring consists of 6 trapezoidal (wrapper) or 80° ring sector (clad) plate elements. Compared to the analytical integration a parametric study shows that a low order numerical integration of the element matrices is sufficient. The resulting linear equation for the displacements of the corner points is solved by a modified Gauss' Algorithm which uses the sparsity of the stiffness matrix for saving central store capacity. By these means the codes requires only 60 K Bytes central store. The code calculates the thermal and neutron swelling strains and the resulting displacements and stresses. The creep strains are calculated iteratively for each time step. External forces induced by pressure, fixed or flexible supports are taken into account and may be changed during the irradiation time.

3. Results. — The code has been used to investigate the behavior of pins and wrapper tube in the planned KNK-II carbide element under various loading conditions and with different swelling formulas. The main outcome of the calculations are: 1) The inherent uncertainly of the swelling formulas lead to very different results for the upper and lower boundary of the swelling formula. 2) In wrapper tubes of cold worked materials which show high swelling at low temperatures the temperature and swelling induced bowing moments interfere in that way that the end deflections are constant or even decreasing with time if the wrapper tube is clamped below and above the core.

The results are compared with results of another code and are in good agreement. The new results obtained with this code are:

1. It is possible to build a mathematical model for the wrapper tube and the cladding tube by using entirely finite elements.
2. The big linear equations may be treated with moderate central store (60 K Bytes).
3. The results of the code are in good agreement with other codes.

1. Problem

The behaviour of a fuel element in pile is not the sum of the behaviour of its parts. As an example: the neutron flux distribution and the cooling channel temperatures influence the themomechanical behaviour of the fuel pin. In the case of an edge pin which is subjected to big azimutal temperature gradients the pin may bow and thus change the cooling channel geometry and acts on to the spacer grids. Therefore fuel pin mechanics, thermohydraulics spacer and wrapper tube mechanics are strongly interconnected and should be represented as one mathematical model.

However the geometrical forms of the individual parts of a fuel bundle and the mathematics for mechanics, hydraulics and thermal conduction are different. Therefore the method of Finite Elements is useful to build such a fuel element, because all geometrical forms may be handled and all types of differential equations may be solved by it. As a first step the method is applied to the mechanics of the wrapper tube and the fuel cladding as they both are slim tubes and behave in a similar way.

2. Method of Solution

The axial and azimutal extent of wrapper and cladding are much bigger than their radial thickness. Therefore, the subdivision of the tubes is done only along the first two directions (fig.1) and the tubes are represented by a stack of hexagonal or circular rings. For simplicity the circular ring of the cladding is simulated by a dodekagon and the wrapper by a hexagon (fig. 2). The basic element for both tubes then is an eightpoint-element E^o with trapezoidal cross section in the x-y-plane and rectangular form in the other planes. The trapezoidal angle of 60^o and 75^o respectively is the main difference between the two elements.

Basic element matrices

The basic element with trapezoidal cross section (fig.3) has 8 points. According to Zienkiewicz /1/ the cartesian x,y,z-corrdinate system is transformed with

$$\begin{aligned} x &= x_o \xi \quad (1 - \zeta s_o / x_o) \\ y &= y_o \eta \\ z &= z_o \zeta \end{aligned} \tag{1}$$

into a coordinate system where the eight corner points are represented by:

$$\begin{aligned} \xi_i &= 1111 \ \bar{1}\bar{1}\bar{1}\bar{1} \\ \eta_i &= 11\bar{1}\bar{1} \quad 11\bar{1}\bar{1} \\ \zeta_i &= 1\bar{1}\bar{1}1 \ 1 \quad 1\bar{1}\bar{1}1 \ 1 \end{aligned} \tag{2}$$

In this ξ,η,ζ coordinate system the basic functions N_i (ξ, η,ζ) assume the simple form

$$N_i = \frac{1}{8} (1 - \xi\, \xi_i) \ (1 + \eta\, \eta_i) \ (1 + \zeta\, \zeta_i) \tag{3}$$

and have the property

$$N_i \ (\xi_j, \eta_j, \zeta_j) = \delta_{ij} \tag{3a}$$

The main equation connecting the element corner displacements $(\delta) = (\delta_{xi}, \delta_{yi}, \delta_{zi})$ and the point forces - the load vector F - is

$$(K) \ (\delta) = (F) \tag{4}$$

The stiffnes matrix K is represented by the volume integral

$$K = \int_{-1}^{1}\int\int\int \ (B^T) \ (D) \ (B \ (x(\xi,\eta,\zeta), \ \ldots) \ ) \ \det \ (J) \ d\xi \ d\eta \ d\zeta \tag{5}$$

where (J) is the Jacobian of the transformation $x,y,z \rightarrow \xi, \eta, \zeta$ and (B) is the strain matrix:

$$( ) = \begin{matrix} \varepsilon_x \\ \varepsilon_y \\ \varepsilon_z \\ \\ xy \\ yz \\ zx \end{matrix} = (B)\ ( ), \qquad (B) = \begin{vmatrix} \partial_x N_i & 0 & 0 \\ 0 & \partial_y N_i & 0 \\ 0 & 0 & \partial_z N_i \\ \partial_y N_i & \partial_x N_i & \\ 0 & \partial_z N_i & \partial_y N_i \\ \partial_z N_i & 0 & \partial_x N_i \end{vmatrix} \qquad (6)$$

(7)

(D) is the elasticity matrix:

$$(D) = \frac{E(1-v)}{(1+v)(1-2v)} \begin{vmatrix} 1 & v_1 & v_1 & & & \\ v_1 & 1 & v_1 & & 0 & \\ v_1 & v_1 & 1 & & & \\ & & & v_2 & & \\ & 0 & & & v_2 & \\ & & & & & v_2 \end{vmatrix} \qquad \begin{aligned} v_1 &= \frac{v}{1-v} \\ v_2 &= \frac{1-2v}{2(1-v)} \end{aligned} \qquad (8)$$

The internal point forces (F^i) generated by thermal ε_o^{th} swelling ε_o^{sw} and creep strains ε_o^{cr} are calculated according to:

$$(F_\varepsilon) = (F_o)\ (\varepsilon_o) = \int_{-1}^{+1}\int\int (B^T)\ (D)\ \det\ (J)\ d\xi\ d\eta\ d\zeta \qquad (\varepsilon_o^{th} + \varepsilon_o^{sw} + \varepsilon_o^{cr}) \qquad (9)$$

The evaluation of both volume integrals is done with a 2x2x2 point Gaussian integration formula which gives no error compared to the analytical integration as the integrands have only therms of power 3 (k) and 2 (F) in ξ, η and ζ.

Hexagonal ring matrices

The basic element matrices represent only the mechanical properties of a trapezoidal block extended in the x-y-plane. corresponding to the element E^o in fig. 2. One way to get the other matrices is to transform the basic matrices with the rotation matrix T:

$$(T) = \begin{vmatrix} \cos\phi_i & 0 & \sin\phi_i \\ 0 & 1 & 0 \\ -\sin\phi_i & 0 & \cos\phi_i \end{vmatrix} \qquad \phi_i = \begin{cases} 60^o \times 1\ 2\ ..\ \text{(wrapper)} \\ 30^o \times 1\ 2\ ..\ \text{(clad)} \end{cases} \qquad (10)$$

If the basic matrix K^o which is of the form 8x3x8x3 (8 points with 3 coordinates) is rearranged as a 3x8x8x3 matrix the matrices K^i of the rotated elements are

$$(K^i) = ((T^T)\ i)\ (K^o)\ (\ (T)\ ^i) \qquad (11)$$

In the same way the internal load vector for these elements may be deduced from the basic one:

$$(F_i) = (\ (T)^i)\ (F_o) \qquad (12)$$

The summation of all relevant matrix components in each point and coordinate of the ring element then gives the matrices (K^{Hex}) and (F^{Hex}) for the hexagonal ring. In the case of the cladding the points at = 30^o, 90^o, ... are suppressed by substructuring in order to reduce the number of degrees of freedom. For the same reason the right side coordinates in fig. 2 are eliminated by substructuring with the assumption of equal strains in opposite elements. That means summetry according to the y-z-plane and only a slight restriction in usefulness as the most problems in wrapper and clad mechanics have at least this symmetry.

System matrices

Each matrix of a hexagonal ring between the planes i and i+1 has the form

$$({}_{K}Hex,i) = \begin{matrix} K_{ii} & C_{ii+1} \\ C^{T}_{i+1i} & K_{i+1i+1} \end{matrix} \qquad (13)$$

where $C^{T}_{ii+1} = C_{i+1i}$ because K is always symmetric. The assemblation of the system matrix for the long wrapper tube or clad would result in a matrix (fig.4) with many zeros because no direct connection exists between distant rings. To avoid waste of central storage only the relevant matrices (K_{ii}) and (C_{ii+1}) are stored in peripheral storage devices.

Before solving the system equation the external forces induced by pressure and supports must be incorporated. The latter may be of two kinds:
Firstly the displacement of some coordinates are predefined. If they are zero the simplest way is to omit the row and column of this coordinate in the system matrix K. If they are not, the product between these coordinate and the respective column of the system matrix is subtracted from the load vector before omitting the row and column of this coordinate. The disadvantage of this method is the varying bandwidth of the system matrix K resulting in a more complex solution scheme.

The second simpler way to incorporate external constrains is to add springs to the system (fig.5). The spring sonstants D_j (kp/mm) are added to the system matrix

$$K'_{jj} = K_{jj} + D_j \qquad (14)$$

at the location j and the coordinate x,y or z. The advantage of this method is doublefold: Firstly the bandwidth of the system matrix stays constant and secondly the support forces may be derived from the "constrained" coordinate displacements:

$$F_i = D_j \ \delta_{xj} \text{ or } \delta_{yj} \text{ or } \delta_{zj} \qquad (15)$$

The system matrix (K') (δ) $= (F)$ which is a hyper matrix with the elements (K'_{ii}) and (C_{ii+1}) is solved by diagonalizing like a normal matrix: (16)

$$(K''_{i+1\ i+1}) = (K'_{i+1\ i+1}) - ((C^{T}_{ii+1})\ (K'^{-1}_{ii})\ (C_{i\ i+1}) \qquad (17)$$

$$0 = (C''_{i+1i}) = (C_{i+1,i}) - ((C^{T}_{i\ i+1})\ (K'^{-1}_{ii}))\ (K'_{ii}) \qquad (18)$$

$$(F''_{i+1}) = (F_{i+1}) - ((C^{T}_{i\ i+1})\ (K'^{-1}_{ii}))\ (F'_{i}) \qquad (19)$$

After this procedure the displacements in the top plane are

$$(\delta^{(n)}) = (K''^{-1}_{nn})\ (F''_{n}) \qquad (20)$$

and of the lower plane:

$$(\delta^{(i)}) = (K''^{-1}_{ii})\ (\ (F''_{i}) - (C_{i\ i+1})\ (\ \delta^{(i+1)})\ ) \qquad (21)$$

After calculating the displacement field (δ_i) the strains ε^{e} in the elements are given by (6) and the stresses by

$$(\sigma^{e}) = (D)\ (\ (B)\ (\delta) - (\varepsilon_{o})\ ) \qquad (22)$$

The creep and swelling formulas are at present taken from /2/.

The program KASTEN is written in the computer language APL. This has some advantages in the build-up and test phase of the program since this language is conceived for interactive use and has very powerful operators for the handling of matrices. One drawback of the APL-system is the rather limited central storage of 64K Bytes. Therefore, the File-system in APL-PLUS was applied to store all big matrices in background storage devices. By this method the program can handle up to 35 subdivisions of a tube which is equivalent to 648 degrees of freedom but is restricted to symmetrical problems as mentioned. The need for peripheral storage in this case is about 1 M Byte and the central processing time on a IBM 158 is 10 sec for one time step.
The calculation of the system matrix is done only one time and needs about 30 seconds. The inversion of the system matrix is done only after altering the support characteristics and needs again 30 seconds.

3. Results

The Karlsruhe KNK-II is a sodium cooled testreactor with fast neutron flux. It is planned to irradiate a carbide bundle in the test zone of this reactor up to 70 000 MWd/kg or 360 days. The neutron flux and temperature gradients are considerable because of the low extent of the core region and may induce stresses and deflections in all bundle elements. Firstly the code KASTEN is used to asses the influence of swelling formula uncertainty on the bundle behaviour.

According to /3/ the swelling of the wrapper material steel No. 14981 which is equivalent to that of No. 14970 may be predicted by a most probabilistic and a pessimistic formula. The behaviour of a wrapper tube with 360°C at the foot, 155° average temperature increase and 60° azimutal temperature difference at core outlet was calculated with these two formulas. The temperature and fast flux in the hot and cold side of the wrapper shows fig. 6 The azimutal flux and temperature gradient results in rather different swelling strains in the hot and cold side in the case of pessimistic swelling. Because at EOL the fast fluence is still rather low, the maximum swell strains differ only slightly, whereas the location of the maximum is shifted 100 mm in the upper direction for the pessimistic swelling formula (fig.7).

The wrapper is clamped at the foot, at the mid of the lower blanket and at the head. The resultant bowing at BOL is low and does not exceed 0,5 mm to the hot side (fig.8 + 9). At MOl this bowing is reduced mainly by irradiation induced creep (thermal creep was neglected because temperatures and stresses are low in this case). AT EOL the point of maximal bowing has shifted towards the lower blanket, but only in the case of pessimistic swelling it reaches again the initial maximum.

The axial stresses (10 + 11) in the cold side at BOL and MOL are similar for both cases. At EOL the axial stress in the pessimistic case is 12 kp/mm^2 compared to 8 kp/mm^2 in the optimistic case. This is caused by the higher swelling yield of this formula at low temperatures. By the same mechanism the tangential stresses (12+13) in the cold side at EOL are higher in the optimistic case. The small positive and negative peak at the begin and at the end of the core region for BOL are due to the steep axial gradient of the tmeperature. In the cold side of the wrapper (fig.14+15) these stresses are higher in magnitude but show a sharp decrease just above the lower support at the lower blanket.

The axial creep strains (16 + 17) are in good agreement at Mol. At EOL they are higher in the optimistic case because the stresses are higher.

In 1971/72 a small axide fuel bundle of the Gesellschaft für Kernforschung was irradiated in the french RAPSODIE reactor. The bowing of the pins were measured after 10 % burnup. Three corner pins with the same environmental conditions (fig. 18) show a simular bowing behaviour. In the cold condition at EOL the bowing is oriented in the direction of the cold temperatures (outside) because the spacer grids suppress any bigger bowing in the hot condition and stresses due to different swelling and thermal expansion are mainly reduced by creep. Thus after cooling down the hot pin side has contracted more than the cold one and bowing is directed in the earlier cold direction. A calculation of the bowing curve with the program KASTEN in the dodekagonal form gives quite good agreement in direction, magnitude and form of the bowing (fig. 18). The temperatures and the fast flux in the pin is shown in fig. 19. The calculated different swelling strains in the hot and cold side at EOL cause rather high stresses in the cladding (fig. 20). If the spacer grid is removed and the pin may bow as shown in fig. 18 the stresses relax only slightly in the core region. The high stresses may be reduced if thermal creep is taken into account. The creep strains are reaching 0,4 % in the core region (fig. 21) and follow the pattern of the stress curve.

References:

/1/ Zienkiewicz, The Finite Element Method in Engeneering Science, 1971 McGraw-Hill, London

/2/ Capart, et al., Design Implications of Material Properties on LMFBR Fuel Elements, ENS-Conference on Nucl. Maturity,'75, Paris

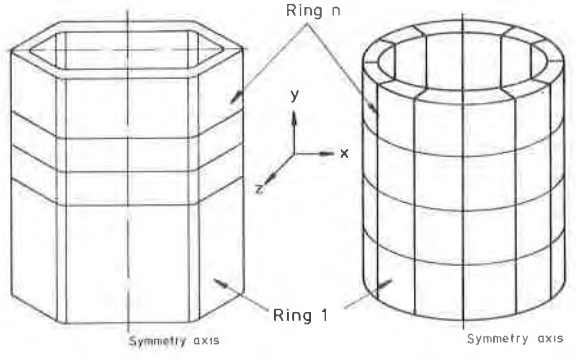

Fig. 1a : Subdivision of wrapper tube

Fig. 1b : Subdivision fo cladding tube

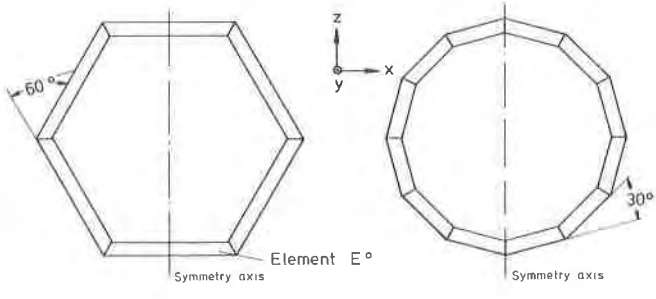

Fig. 2a : Cross section of finite elements for the wrapper model

Fig. 2b : Cross section of finite elements for the cladding model

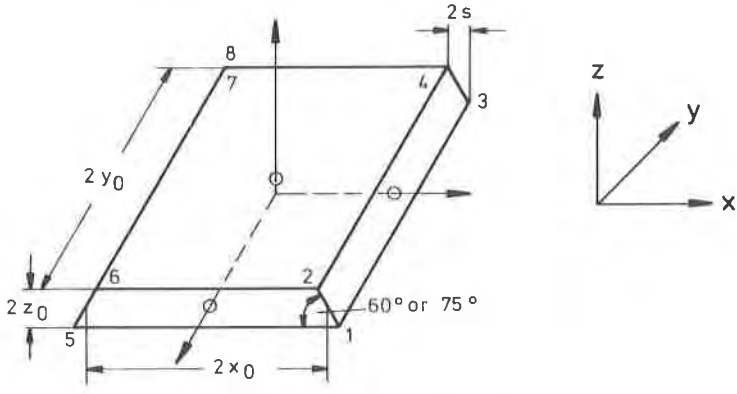

Fig. 3 : Trapezoidal block element

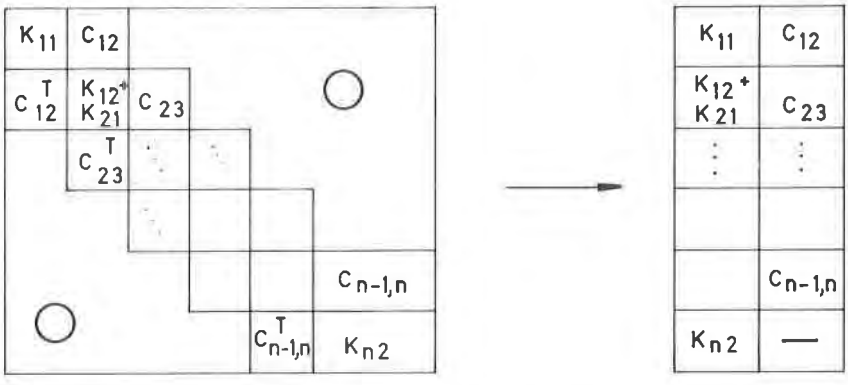

Fig. 4 : System matrix storage scheme

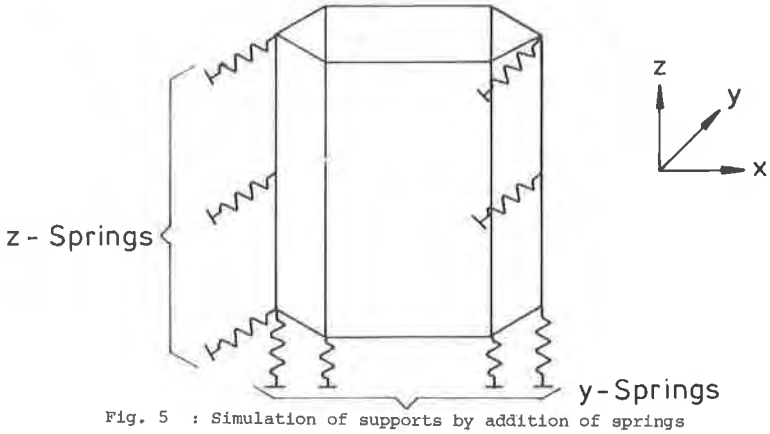

Fig. 5 : Simulation of supports by addition of springs

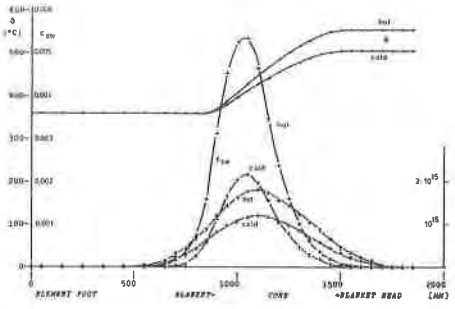

Fig. 6 : Temperatures, fast flux and swelling strains at EOL (pessimistic case) in the hot and cold side of the KNK II carbide wrapper

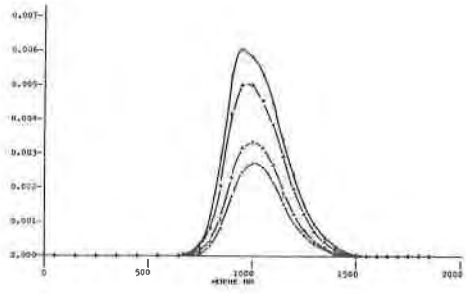

Fig. 7 : Swelling strains at EOL (optimistic case)

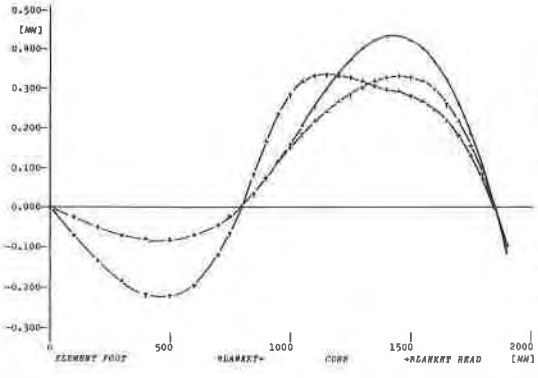

Fig. 8 : Deflection of wrapper tube at BOL (.), MOL (+) and EOL (+) (pessimistic case)

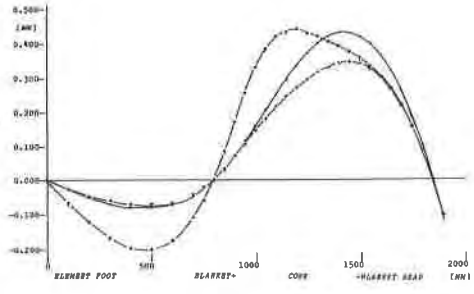

Fig. 9. : Deflections of wrapper tube at BOL (.), MOL (+) and EOL (+) (optimistic case)

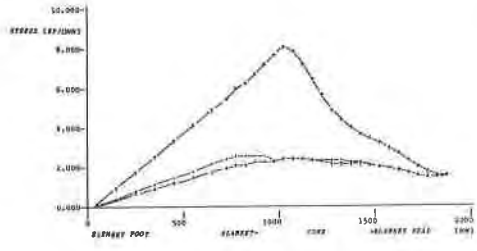

Fig. 10 : Axial stresses in the cold side at BOL (.), MOL (+) and EOL (+) (pessimistic swelling formula)

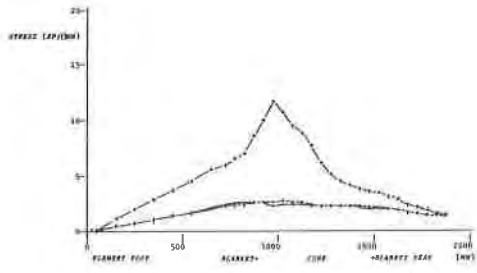

Fig. 11 : Axial stresses in the cold side at BOL (.), MOL (+) and EOL (+) (optimistic swelling formula)

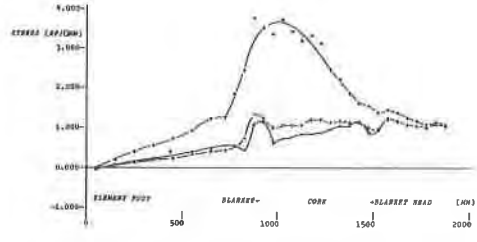

Fig. 12 : Tangential stresses in the cold side at BOL (.), MOL (+) and EOL (+) (pessimistic swelling formula)

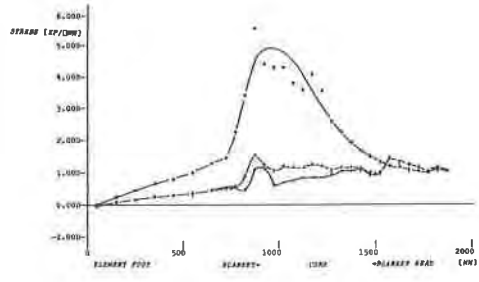

Fig. 13 : Tangential stresses in the cold side at BOL (.), MOL (+) and EOL (+) (optimistic swelling formula)

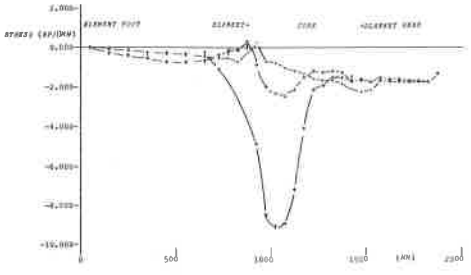

Fig. 14 : Tangential stresses in the hot side at BOL (.), MOL (+) and EOL (+)
(pessimistic swelling formula)

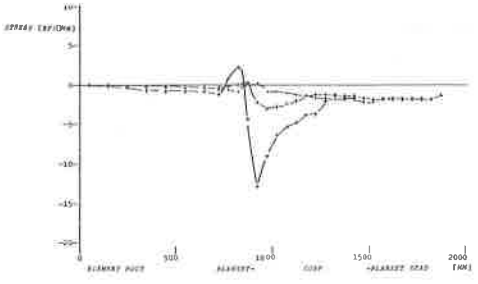

Fig. 15 : Tangential stresses in the hot side at BOL (.), MOL(+) and EOL (+)
(optimistic swelling formula)

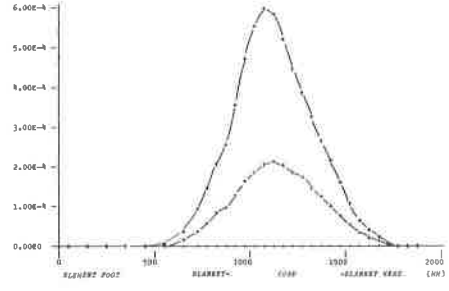

Fig. 17 : Axial creep strains at BOL (.), MOL (+) and EOL (+)
(optimistic swelling formula)

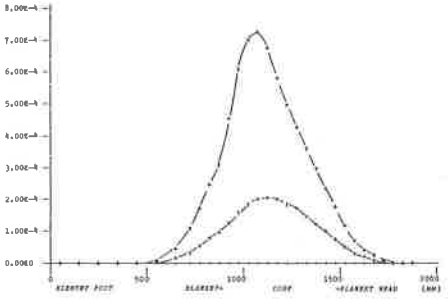

Fig. 16 : Axial creep strains at BOL (.), MOL (+) and EOL (+)
(pessimistic swelling formula)

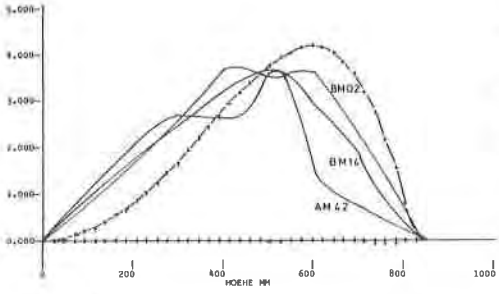

Fig. 18 : Comparison of pin bowing after 10 % burn-up, cooling down and removing all distance grids at EOL (-)experimental curve, (+)theoretical

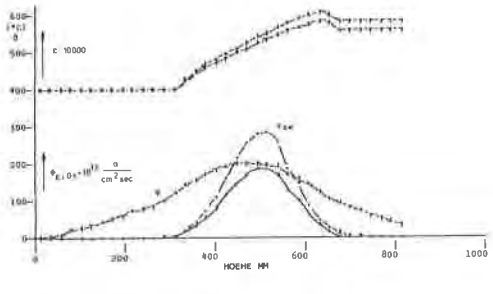

Fig. 19: Temperatures (+), swelling strains (·) and flux (+) in the pins AM 42, BM 14 and BM 02 of the rapsodie experiment

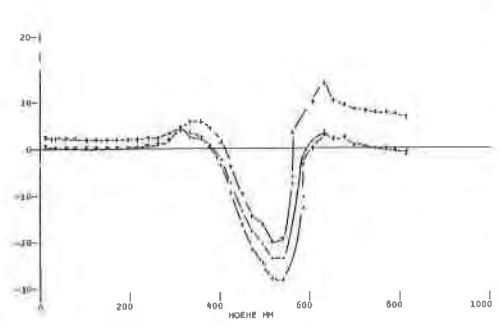

Fig. 20: Axial stresses in the hot side at 350 days (·), 365 days (+) hot and 365 days cold (+)

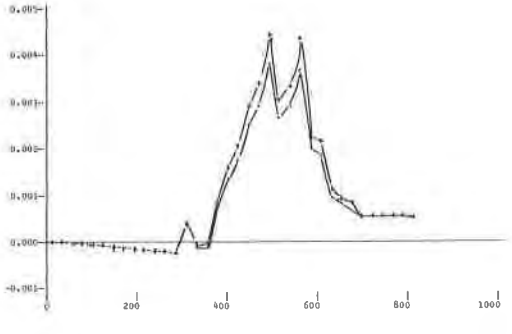

Fig. 21: Axial creep strains in the cold side at 350 days (·) and 365 days (+)